JACS
JOURNAL OF THE AMERICAN CHEMICAL SOCIETY

Communication

pubs.acs.org/JACS

Superomniphobic Magnetic Microtextures with Remote Wetting Control

Anton Grigoryev,[†] Ihor Tokarev,[†] Konstantin G. Kornev,[‡] Igor Luzinov,[‡] and Sergiy Minko*,[†]

[†]Department of Chemistry and Biomolecular Science, Clarkson University, 8 Clarkson Avenue, Potsdam, New York 13699, United States

[‡]School of Materials Science and Engineering, Clemson University, 263 Sirrine Hall, Clemson, South Carolina 29634-0971, United States

Supporting Information

ABSTRACT: Universal remote control of wetting behavior enabling the transition from a superomniphobic to an omniphilic wetting state in an external magnetic field via the alternation of reentrant curvature of a microstructured surface is demonstrated. This reconfigurable microtexture made of Ni micronails repels water, water−surfactant solutions, and practically all organic liquids, whereas it gets wetted by all of these liquids after a magnetic field pulse is applied.

The ability to manipulate liquid droplets is crucial for the generation of super-repellent materials, including protective gear, solid−liquid interfaces with minimum-to-maximum liquid drag, and logic gates for microfluidic analytical devices.[1−3] Here we show unprecedented and universal remote control of wetting behavior enabling the transition from a superomniphobic to an omniphilic wetting state in an external magnetic field via the alternation of reentrant curvature of a microstructured surface. This specially designed reconfigurable microtexture made of ferromagnetic metal micronails repels water, water−surfactant solutions, and practically all organic liquids (besides fluorinated solvents), including such superspreading amphiphiles as tributyl phosphate and alcohols. This superomniphobic state can be turned into an omniphilic one by applying magnetic field.

It is a well-established fact that roughness alters the wettability of solid surfaces, leading to either the Wenzel or Cassie−Baxter regimes.[4] In the former regime, the liquid fully fills the surface cavities, while in the latter case, the liquid shows limited penetration into the surface cavities, trapping air bubbles underneath the droplet. For rough or textured surfaces, the Cassie−Baxter regime can be observed for nonwettable materials (in this case, a liquid droplet beads up on a smooth surface of the same material if the equilibrium contact angle is greater than 90°). In particular, this regime can be straightforwardly realized for water in contact with hydrophobic materials. Properly textured hydrophobic materials exhibit superhydrophobic properties defined by apparent contact angles of >150°.[2,5−10] However, the composite wetting state cannot be easily achieved for liquids with lower surface tension, such as organic solvents and oils. It is especially true for low-surface-tension liquids (e.g., decane and ethanol), for which no material with an equilibrium contact angle of >90° is known. Such liquids spread on smooth or textured surfaces and produce the thermodynamically stable Wenzel state. This difficulty has been overcome by making specially engineered surfaces with topographic features having overhang or reentrant geometry, such as micronail forests, microhoodoo arrays, woven textiles, fiber mats, and nanoparticle coatings.[11−21] Such reentrant textures can be designed to support the composite wetting regime for liquids having a wide range of surface tensions, from water (γ = 72.8 mN m^{-1}) down to alcohols and alkanes. Textured surfaces with apparent contact angles of >150° for both water and oil are called superlyophobic or superomniphobic surfaces. Reentrant omniphobic (nonwettable) surfaces are characterized by overhangs or reentrant angles and must obey a set of guidelines and rules that have recently been formulated to aid their structural design.[13,16,22−24]

Only a few studies have demonstrated reentrant textures that repel liquids with surface tensions lower than that of hexadecane (γ = 27.5 mN m^{-1}). This scarcity of experimental studies is rationalized by the difficulties associated with fabricating reentrant textures with efficient and robust liquid-repellent geometries. The combination of photolithography, SiO_2 deposition, and a two-step etching process was employed to produce periodic silicon-based microstructures consisting of undercut pillars with overhung flat caps (termed microhoodoos).[12−14] These T-shaped microfabricated structures exhibit robust superlyophobicity for liquids with surface tensions as low as that of pentane (γ = 16.1 mN m^{-1}).[13]

In this work, we have developed an approach in which template-assisted electrodeposition is used to produce arrays of high-aspect-ratio Ni wires topped with micrometer-sized hemispherical caps (termed hereafter micronails). We used 30−60 μm track−etch polycarbonate membranes having uniform cylindrical pores with diameters of ca. 2 μm and a pore density of 7 × 10^4 cm^{-2} as sacrificial templates for the synthesis of the Ni micronails (Figure 1a). Polycarbonate foils (30 and 60 μm in thickness) were irradiated with heavy ions at the UNILAC linear accelerator of GSI Helmholtzzentrum für Schwerionenforschung GmbH (Darmstadt, Germany). The exposure resulted in the formation of continuous ion tracks in the polycarbonate in the direction normal to the foil surfaces. The irradiated foils were treated with a 5 M NaOH aqueous

Received: June 2, 2012

   dx.doi.org/10.1021/ja305348n | J. Am. Chem. Soc. XXXX, XXX, XXX−XXX

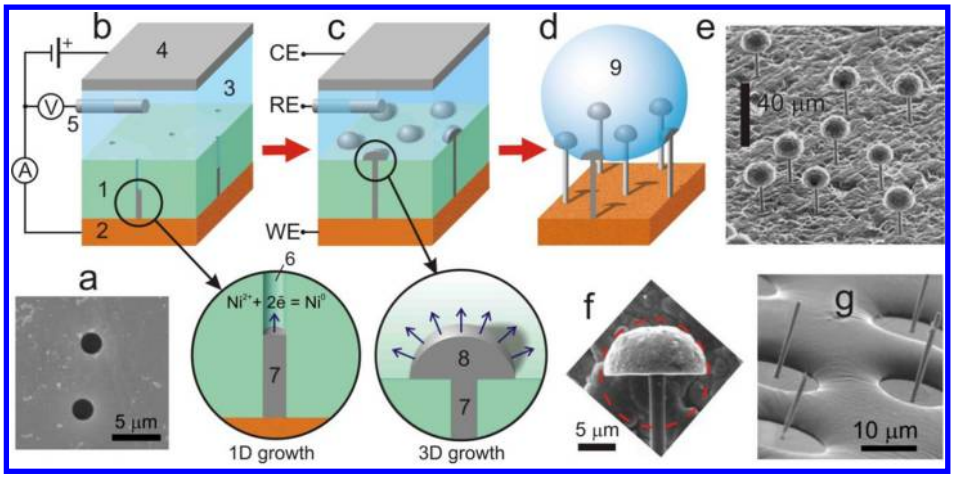

Figure 1. Fabrication and characterization of a Ni micronails. (a) SEM micrograph of a polycarbonate template. (b) Three-electrode electrodeposition setup consisting of a track–etch template (1), a metal working electrode (WE) deposited on one side of the template (2), a Ni electroplating bath (3), a Ni counter electrode (CE) (4), and a reference electrode (RE) (5). The enlarged schematic shows the pore-confined 1D growth of Ni in a template pore (6), resulting in the formation of a Ni wire leg (7). (c) Ni wires reach the top of the template and continue to grow. The enlarged schematic shows the unrestricted 3D growth of Ni on the template surface, resulting in the formation of a hemispherical cap (8). (d) The structure after removal of the template consists of a bed of Ni micronails and supports the Cassie–Baxter regime (9). (e) SEM image of a cluster of electrodeposited Ni micronails. (f) Zoomed-in SEM image of a single micronail with a hemispherical cap. (g) SEM image demonstrating the Cassie–Baxter state for an epoxy resin droplet sitting on a bed of Ni micronails. The micronails were separated from the metal substrate to visualize the reverse side of the droplet. The pinning of the droplet to the cap's ridge and its sagging between the micronails are clearly visible; the sagging depth is much smaller than the micronail height.

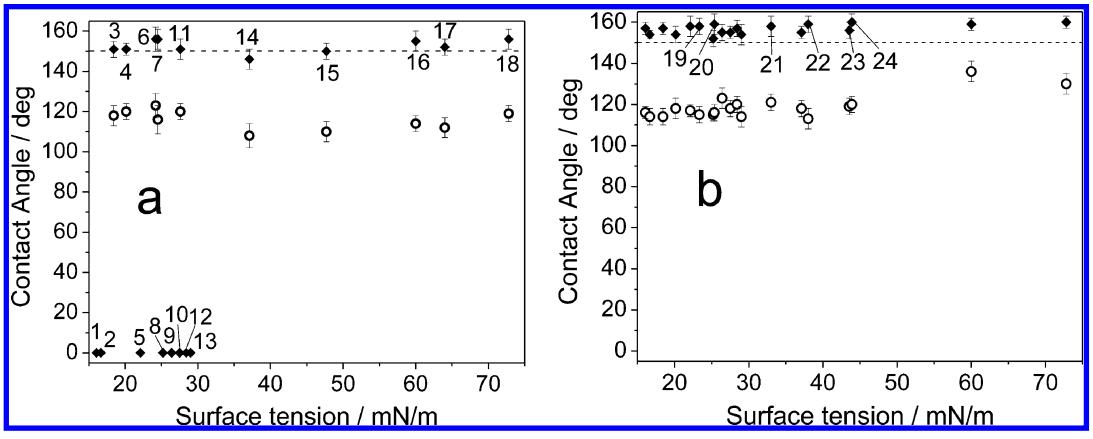

Figure 2. Advancing (◆) and receding (○) contact angles as functions of liquid surface tension for different liquids on a surface of Ni micronails with a cap radius of 5 μm at 20 °C (a) before and (b) after its modification with fluoroalkylthiol. Legend: 1 – pentane, 2 – ethyl ether, 3 – hexane, 4 – heptane, 5 – ethanol, 6 – butanol, 7 – hexanol, 8 – acetone, 9 – tetrahydrofuran, 10 – chloroform, 11 – octanol, 12 – toluene, 13 – tributyl phosphate, 14 – DMF, 15 – ethylene glycol, 16 – 1% aqueous SDS solution, 17 – glycerol, 18 – water, 19 – propanol, 20 – dodecane, 21 – 1,4-dioxane, 22 – pyridine, 23 – dimethyl sulfoxide, and 24 – nitrobenzene. See Table S1 in the SI for details.

solution containing 10 vol % methanol at 50 °C for 30 min for chemical etching of the tracks. The etched foils were washed in a 10:1 (v/v) water/methanol mixture for 2 h and air-dried.

Ni wires were electrochemically grown within the pores of the polymer template, one side of which was covered with gold (99.99%) by sputter coating to create a 1 μm thick conductive electrode (Figure 1b). In addition, a thick layer of copper was electrochemically grown on top of the gold electrode to increase its total thickness, so that it could mechanically support the Ni micronails. Prior to the Ni electrodeposition, the electrode (cathode) was equipped with an external contact, and the electrode's open areas (except those accessible through the pores) were insulated to protect them from contact with the electrolyte. The deposition of Ni was performed through pores of the template in a potentiostatic regime (−1 V vs Ag/AgCl) in an aqueous plating bath (pH 3.7) containing 150 g L^{-1} $NiSO_4 \cdot 6H_2O$, 60 g L^{-1} $NiCl_2 \cdot 6H_2O$, 37 g L^{-1} saturated H_3BO_3 (filtered), and 10 vol % ethanol. The deposition current was used to monitor the filling of the template with Ni. A weak increase in the current was observed as Ni filled the cylindrical pores of the template. The pore confinement led to the formation of Ni wires in the template (Figure 1b). As the wire tips reached the top of the template, the Ni growth was not restricted by the pore walls anymore, and the growth mode changed from anisotropic to three-dimensional (3D) (Figure 1c). As a result, hemispherical Ni caps formed on the template surface (Figure 1f), and their size increased with increasing deposition time. The current exhibited a rapid increase in this mode, indicating the 3D growth of the caps. The cap size was correlated with the deposition current, which allowed us to control the deposition process and cease it when a target cap diameter (between 4 and 8 μm) was reached. Dissolution of the

dx.doi.org/10.1021/ja305348n | J. Am. Chem. Soc. XXXX, XXX, XXX–XXX

template in dimethylformamide (DMF) uncovered a microstructure consisting of a bed of Ni micronails on the electrode surface [Figure 1e and Figure S1 in the Supporting Information (SI)]. The nickel surface was cleaned with an oxygen plasma to remove any traces of polycarbonate. The micronails on the electrode surface were randomly positioned (because of the random distribution of pores in the polymer template) and for the most part well-separated.

Contact angle analysis of the Ni micronail surfaces with no additional surface modification revealed that they support the Cassie–Baxter regime with apparent contact angles of >150° (and thus demonstrate superomniphobic properties) with a broad range of liquids, including water, aqueous solutions of sodium dodecyl sulfate (SDS), plant oil, tributyl phosphate, and numerous nonpolar and polar organic solvents. It has to be noted that some of these liquids (e.g., organic solvents) readily wet the smooth, untreated Ni surface, exhibiting contact angles of <10°. Figure 2a shows the advancing and receding contact angles of the liquids on the bed of micronails as functions of the liquid surface tension. In the case of nonpolar alkanes, the Cassie–Baxter state is observed for hexane (γ = 18.4 mN m^{-1}) and other alkanes with higher surface tension. We are not aware of other experimental studies demonstrating superomniphobic behavior for liquids with surface tensions as low as that of hexane on textured surfaces made of an intrinsically wettable material. On the other hand, we found that pentane, an alkane with a surface tension lower than hexane, was imbibed by the Ni microtexture, producing the Wenzel state. In the case of polar alcohols, the forest of micronails repelled butanol (γ = 24.2 mN m^{-1}) and other alcohols with higher surface tensions, whereas it allowed the penetration of ethanol (γ = 22.1 mN m^{-1}). As exemplified by alkanes and alcohols, it follows that the threshold surface tension at which the Cassie–Baxter state transitions to the Wenzel regime differs for different groups of liquids. This result demonstrates that the wetting properties of the surface cannot be linked to a single parameter (i.e., γ) and that polar interactions of the liquid with the solid surface have to be taken into account.

The wetting behavior changed after the micronails were coated first with gold and then with a self-assembled monolayer (SAM) of 1*H*,1*H*,2*H*,2*H*-perfluorodecanethiol from a 1 mM solution in hexane for 24 h. The surface modification led to a considerable decrease in the surface energy of the microtexture and also eliminated the polar component of the liquid–solid (L–S) interactions. In this case, the wetting regime was solely defined by the liquid surface tension (Figure 2b). Thus, the fluorinated micronail structures supported the Cassie–Baxter state for isopentane (γ = 15.0 mN m^{-1}), pentane (γ = 16.1 mN m^{-1}), and other nonpolar and polar liquids with higher surface tension. This result also comparable to that obtained for the periodic microhoodoo geometry, for which the Cassie–Baxter regime was observed for liquids with surface tensions as low as that of pentane.[13] However, no measurements have been reported for liquids with γ < 15 mN m^{-1} (isopentane and pentane are the last in the series of alkanes that are liquids). Our measurements showed that perfluorooctane (a fluorocarbon liquid with γ = 14 mN m^{-1}) impregnated the micronail texture, resulting in the Wenzel state (see the discussion and calculations in the SI).

Manipulation of liquid droplets and control of liquid transport and adhesion could be realized through control of the wetting transition (switching) from liquid-repellent to wetting behavior. Switchable superhydrophobic textured surfaces have been reported in many recent studies[25] employing switching of chemical composition[25b] or surface microstructure.[25c,d] In particular, external fields have been used to approach remote wetting control. For example, an external magnetic field was used to bend polymeric tubes with incorporated magnetic nanoparticles and hence decrease the contact angle of water to 102° from the initial value of 117°. Water remained in the Cassie–Baxter regime when the magnetic field was applied because the wetting mechanism was not changed through the actuation process.[26]

In contrast to those results, only a few examples of switchable superomniphobic textured surfaces exist.[11] Electrically switchable superomniphobic surfaces composed of T-shaped features were used to induce the nonwetting-to-wetting transition.[11] The experimental setup required voltages on the order of tens to a few hundreds of volts and an electrode inserted into a liquid droplet. Furthermore, there is a limit on the extent to which the contact angle can be lowered by the electric potential, known as contact angle saturation.[27,28]

Universal remote control of wetting behavior by switching from the Cassie–Baxter to Wenzel regime was realized in the present work. The transition between these two wetting mechanisms was achieved by forcing the caps of the T-shaped features to bend to a reentrant angle exceeding the equilibrium contact angle of the liquid (Figure 3a,b). In our system, a magnetic field (50 mT) was used to bend Ni micronails (Figure 3c,d) and thus induce the transition from the nonwetting Cassie–Baxter state to the wetting Wenzel state. We found that

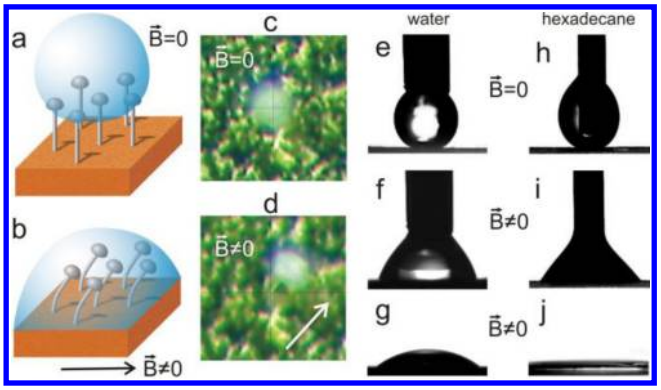

Figure 3. Magnetically induced nonwetting-to-wetting transition. (a) A bed of vertical micronails supports a liquid in the Cassie–Baxter state. (b) Bending of the micronail caps by an external magnetic field from the upright position (0°) to an angle exceeding the equilibrium contact angle of the liquid for a given material causes spontaneous imbibition of the liquid into the microstructure and the formation of the fully wetting Wenzel state. (c, d). Optical micrographs showing bending of an individual Ni micronail (leg length of 60 μm) in an external magnetic field. The micronail is in the upright position under no field (c) and bends over when a permanent rare-earth magnet is brought into the vicinity of the microstructure, with the cap forming an angle of 23° with the surface normal (d). The cross-hairs (black solid lines) are used to guide the eye in following the change in the micronail geometry. (e–j) Photographic images showing different stages of measurements of the contact angles of (e–g) water and (h–j) hecadecane on a bed of Ni micronails. (e, h) Under no field, the Cassie–Baxter regime is observed, with apparent contact angles of 159° for water and 153° for hexadecane. (f, i) When the magnetic field is applied, the liquids transition to the Wenzel state. (g, j) When the dispensing needle is removed, hexadecane spreads over the surface, exhibiting complete wetting (j), whereas water displays partial wetting on the support surface (g).

dx.doi.org/10.1021/ja305348n | *J. Am. Chem. Soc.* XXXX, XXX, XXX–XXX

only the special design of the micronails with bulky Ni caps at the tips of high-aspect ratio wires led to the ability of the micronails to bend in the external magnetic field to an extent where the reentrant angle was greater than the equilibrium contact angle. Cap-free Ni wires with the same length exhibited no detectable bending or changes in wetting behavior in the aforesaid field. The magnetic-field-induced transition led to dramatic changes in the contact angle, as was demonstrated for two different kinds of liquid: water and hexadecane (Figure 3e–j). The Ni micronail structure with no surface modification was used in the experiments. A dramatic decrease in the apparent contact angles of the two liquids from >150° (superomniphobic state) to much less than 90° was observed when the magnet was brought for a second into the vicinity of the microstructure (Figure 3). Hexadecane showed complete wetting when the dispensing needle was removed. A water droplet showed partial wetting in the Wenzel state when the wetting properties were dominated by the nail-supporting gold substrate or the surface-modified gold substrate (at the low density of nails, they had no substantial impact on wetting in the Wenzel state). Obviously, the superomniphobic property was restored when the microstructure surface was dried.

In summary, we have demonstrated microstructured reentrant surfaces whose wetting behavior can be switched from a liquid-repellent (superomniphobic) state to a wetting state using an external magnetic field by increasing the reentrant angle of the overhang structures from 0° to 23°. These microstructures, composed of 2D random arrays of ferromagnetic micronails with large hemispherical caps, can produce highly robust surfaces supporting the nonwetting Cassie–Baxter state for a broad range of nonpolar and polar liquids. The random lateral allocation of the micronails does not disrupt the ability of the microstructure to repel liquids.

The nonwetting-to-wetting transition due to magnetically induced bending of micronails to change the local geometric angle (reentrant angle) is free of the major limitation inherent in the existing methods of electrically, chemically, and photochemically triggered wetting. Thus, the universal character of this approach is due to changes in the wetting mechanism through reconstruction of the reentrant curvature, where wetting becomes less dependent on the wetting liquid and the wetted surface.

■ ASSOCIATED CONTENT

Ⓢ Supporting Information

SEM images of micronails, contact angles for different liquids, and quantitative estimates of the robustness of the Cassie–Baxter state. This material is available free of charge via the Internet at http://pubs.acs.org.

■ AUTHOR INFORMATION

Corresponding Author

sminko@clarkson.edu

Notes

The authors declare no competing financial interest.

■ ACKNOWLEDGMENTS

The authors acknowledge the NSF for support (CMMI Grants 0825832 and 0825773) and GSI Helmholtzzentrum für Schwerionenforschung GmbH for samples of irradiated polycarbonate films. The authors are grateful for discussions with Professors Michael Rubner and Robert Cohen.

■ REFERENCES

(1) Bocquet, L.; Lauga, E. *Nat. Mater.* **2011**, *10*, 334.
(2) Bhushan, B.; Jung, Y. C. *Prog. Mater. Sci.* **2011**, *56*, 1.
(3) Blossey, R. *Nat. Mater.* **2003**, *2*, 301.
(4) Whyman, G.; Bormashenko, E.; Stein, T. *Chem. Phys. Lett.* **2008**, *450*, 355.
(5) Quere, D. *Nat. Mater.* **2002**, *1*, 14.
(6) Lafuma, A.; Quere, D. *Nat. Mater.* **2003**, *2*, 457.
(7) Liu, K. S.; Yao, X.; Jiang, L. *Chem. Soc. Rev.* **2010**, *39*, 3240.
(8) Li, X. M.; Reinhoudt, D.; Crego-Calama, M. *Chem. Soc. Rev.* **2007**, *36*, 1350.
(9) Dorrer, C.; Ruhe, J. *Soft Matter* **2009**, *5*, 51.
(10) Gao, L. C.; McCarthy, T. J.; Zhang, X. *Langmuir* **2009**, *25*, 14100.
(11) Ahuja, A.; Taylor, J. A.; Lifton, V.; Sidorenko, A. A.; Salamon, T. R.; Lobaton, E. J.; Kolodner, P.; Krupenkin, T. N. *Langmuir* **2008**, *24*, 9.
(12) Tuteja, A.; Choi, W.; Ma, M. L.; Mabry, J. M.; Mazzella, S. A.; Rutledge, G. C.; McKinley, G. H.; Cohen, R. E. *Science* **2007**, *318*, 1618.
(13) Tuteja, A.; Choi, W.; Mabry, J. M.; McKinley, G. H.; Cohen, R. E. *Proc. Natl. Acad. Sci. U.S.A.* **2008**, *105*, 18200.
(14) Tuteja, A.; Choi, W. J.; McKinley, G. H.; Cohen, R. E.; Rubner, M. F. *MRS Bull.* **2008**, *33*, 752.
(15) Choi, W.; Tuteja, A.; Chhatre, S.; Mabry, J. M.; Cohen, R. E.; McKinley, G. H. *Adv. Mater.* **2009**, *21*, 2190.
(16) Chhatre, S. S.; Choi, W.; Tuteja, A.; Park, K. C.; Mabry, J. M.; McKinley, G. H.; Cohen, R. E. *Langmuir* **2010**, *26*, 4027.
(17) Darmanin, T.; Guittard, F.; Amigoni, S.; de Givenchy, E. T.; Noblin, X.; Kofman, R.; Celestini, F. *Soft Matter* **2011**, *7*, 1053.
(18) Fujii, T.; Aoki, Y.; Habazaki, H. *Langmuir* **2011**, *27*, 11752.
(19) Hsieh, C. T.; Wu, F. L.; Chen, W. Y. *Mater. Chem. Phys.* **2010**, *121*, 14.
(20) Zhang, J. P.; Seeger, S. *Angew. Chem., Int. Ed.* **2011**, *50*, 6652.
(21) Steele, A.; Bayer, I.; Loth, E. *Nano Lett.* **2009**, *9*, 501.
(22) Nosonovsky, M. *Langmuir* **2007**, *23*, 3157.
(23) Choi, W.; Tuteja, A.; Mabry, J. M.; Cohen, R. E.; McKinley, G. H. *J. Colloid Interface Sci.* **2009**, *339*, 208.
(24) Marmur, A. *Langmuir* **2008**, *24*, 7573.
(25) (a) Xia, F.; Zhu, Y.; Feng, L.; Jiang, L. *Soft Matter* **2009**, *5*, 275. (b) Minko, S.; Muller, M.; Motornov, M.; Nitschke, M.; Grundke, K.; Stamm, M. *J. Am. Chem. Soc.* **2003**, *125*, 3896. (c) Sidorenko, A.; Krupenkin, T.; Taylor, A.; Fratzl, P.; Aizenberg, J. *Science* **2007**, *315*, 487. (d) Kim, P.; Zarzar, L. D.; Zhao, X. H.; Sidorenko, A.; Aizenberg, J. *Soft Matter* **2010**, *6*, 750.
(26) Zhou, Q.; Ristenpart, W. D.; Stroeve, P. *Langmuir* **2011**, *27*, 11747.
(27) Mugele, F. *Soft Matter* **2009**, *5*, 3377.
(28) Drygiannakis, A. I.; Papathanasiou, A. G.; Boudouvis, A. G. *Langmuir* **2009**, *25*, 147.